Published in final edited form as:
J Neurochem. 2010 March ; 112(6): 1454–1464. doi:10.1111/j.1471-4159.2009.06557.x.

The endogenous cannabinoid, anandamide, inhibits dopamine transporter function by a receptor–independent mechanism

Murat Oz[*,†], **Vanaja Jaligam**[*], **Sehamuddin Galadari**[‡], **George Petroianu**[†], **Yaroslav M. Shuba**[§], and **Toni S. Shippenberg**[*]

[*]Integrative Neuroscience Section, Intramural Research Program, National Institute on Drug Abuse, National Institutes of Health, US Department of Health and Human Services, Baltimore, Maryland, USA

[†]Laboratories of Functional Lipidomics, Department of Pharmacology, UAE University, Al Ain, UAE

[‡]Cell Signaling, Department of Biochemistry and Faculty of Medicine and Health Sciences, UAE University, Al Ain, UAE

[§]Bogomoletz Institute of Physiology, National Academy of Sciences of Ukraine, Kiev, Ukraine

Abstract

The endocannabinoid, anandamide (AEA), modulates the activity of the dopamine transporter (DAT) in heterologous cells and synaptosomal preparations. The cellular mechanisms mediating this effect are unknown. The present studies employed live cell imaging techniques and the fluorescent, high affinity DAT substrate, 4-(4-(dimethylamino)-styryl)-*N*-methylpyridinium (ASP^+), to address this issue. AEA addition to EM4 cells expressing yellow fluorescent protein-tagged human DAT (hDAT) produced a concentration-dependent inhibition of ASP^+ accumulation (IC_{50}: 3.2 ± 0.8 μM). This effect occurred within 1 min after AEA addition and persisted for 10 min thereafter. Pertussis toxin did not attenuate the effects of AEA suggesting a mechanism independent of G_i/G_o coupled receptors. The amidohydrolase inhibitor, phenylmethylsulfonyl fluoride (0.2 mM), failed to alter the AEA-evoked inhibition of ASP^+ accumulation. Methanandamide (10 μM), a metabolically stable analogue of AEA inhibited accumulation but arachidonic acid (10 μM) was without effect suggesting that the effects of AEA are not mediated by its metabolic products. The extent of AEA inhibition of ASP^+ accumulation was not altered in cells pre-treated with 1 μM URB597, a specific and potent fatty acid amide hydrolase inhibitor, and the cyclooxygenase inhibitor, indomethacin (5 μM) Live cell imaging revealed a significant redistribution of hDAT from the membrane to the cytosol in response to AEA treatment (10 μM; 10 min). Similarly biotinylation experiments revealed that the decrease in DAT function was associated with a reduction in hDAT cell surface expression. These results demonstrate that AEA modulates DAT function via a cannabinoid receptor-independent mechanism and suggest that AEA may produces this effect, in part, by modulating DAT trafficking.

Keywords

anandamide; cannabinoids; dopamine transporter; HEK293 cells

The neurotransmitter, dopamine (DA) modulates excitatory and inhibitory neurotransmission in brain regions that control movement, emotion, and reward. Dysregulation of DA

Address correspondence and reprint requests to Toni S. Shippenberg, Integrative Neuroscience Section, NIDA IRP, 333 Cassell Dr., Baltimore, MD 21224, USA. tshippen@intra.nida.nih.gov.

transmission is implicated in the etiology of several pathological conditions including Parkinson's disease, drug addiction, and schizophrenia. The DA transporter (DAT) is an integral membrane protein that is a member of the Na^+- and Cl^--dependent cotransporter gene family (Amara and Kuhar 1993). It serves a key role in regulating pre-synaptic DA transmission by clearing DA released into the extracellular space.

Systemic administration of the endocannabinoid, anandamide (AEA), increases extracellular DA levels in the nucleus accumbens, a brain region implicated in mediating the abuse liability of various psychoactive drugs (Solinas *et al.* 2006). Increased DA levels are also observed in response to synthetic cannabinoid agonists (Fadda *et al.* 2006; Tanda *et al.*, 1997). Although these effects have been attributed to alterations in DA release (Solinas *et al.* 2006), evidence that AEA and other cannabinoids inhibit DA uptake in native tissue and heterologous expression systems has been presented (Chen *et al.* 2003; Steffens and Feuerstein 2004; Price *et al.* 2007; Sidló *et al.* 2008). Such findings are noteworthy in that they suggest that AEA may modulate DA transmission by regulating DAT function.

The cellular mechanisms mediating the interaction of AEA with DAT are unclear. Although there is evidence that AEA may modulate DAT function by a CB1 independent mechanism (Steffens and Feuerstein 2004; Price *et al.* 2007), whether the effect of AEA is mediated by the activation of other cannabinoid receptors such as CB2 and GPR55 (Brown 2007) known to be expressed in brain is unclear. In addition, although prolonged incubation of cells or synaptosomes decreases DA uptake, the time course and the cellular mechanisms of this effect have not been assessed.

Recent studies have demonstrated that use of the fluorescent, high affinity DAT substrate, 4-(4-(dimethylamino)styrl)-*N*-methylpyridinium (ASP^+), in combination with confocal microscopy enables real-time, spatially resolved analysis of DAT function in heterologous expression systems and neuronal cultures. (Schwartz *et al.* 2003, 2006; Mason *et al.* 2005). Analysis of ASP^+ accumulation not only permits resolution of substrate binding and uptake in the same cell but enables quantification of rapid (e.g. ≤ 1 min) changes in DAT function (Bolan *et al.* 2007; Zapata *et al.* 2007). In the present study, we have used the ASP^+ technique to investigate the effect of AEA on the function of human DAT (hDAT) expressed in the EM4 HEK293 cell line which does not endogenously express known cannabinoid receptors (Barann *et al.* 2002; Brown 2007). Using live cell imaging and biotinylation techniques, the influence of AEA on DAT cell surface expression was also assessed.

Methods

Materials

Anandamide was generously provided by NIDA Drug Supply/NIH, Rockville, MD, USA. Pertussis toxin (PTX), methanandamide, arachidonic acid, phenylmethylsulfonyl fluoride (PMSF), A23187 and indomethacin were obtained from Sigma-RBI (St. Louis, MO, USA). URB597 was purchased from Cayman Chemical (Ann Arbor, MI, USA). Anandamide, methanandamide, URB597, and arachidonic acid were dissolved in ethanol at 10 mM stock concentrations and kept at −20°C.

Cell culture

Experiments were conducted in EM4 cells, a HEK293 cell line that stably expresses a macrophage scavenger receptor to increase their adherence to tissue culture plastic (EM4 cells, R.A. Horlick, Pharmacopeia, Cranberry, NJ, USA). Cells were maintained in Dulbecco's modified Eagle's medium /Ham's F-12 medium (50 : 50; Mediatech, Inc., Herndon, VA, USA) supplemented with 10% fetal bovine serum (FBS). They were grown in a humidified

atmosphere at 37°C and 5% CO_2. Twenty four hours after plating, cells were transiently transfected with yellow fluorescent protein-tagged human DAT (YFP-hDAT) using LTX (Invitrogen, Carlsbad, CA, USA) according to the manufacturer's instructions or FLAG-hDAT. Experiments were performed 48 h after transfection when cells were 70–80% confluent. The addition of these tags does not alter transporter-mediated [^{3}H]DA uptake (Saunders *et al.* 2000; Zapata *et al.* 2007).

ASP$^+$ uptake

For ASP^+ experiments, cells were seeded on day 1 at 1.4×10^5 cells/35-mm Delta T Petri dish (Bioptechs, Butler, PA, USA). Between 40 and 70 cells were used for each experiment unless otherwise stated. These cells were pooled from at least three separate transfections, with a minimum of two dishes analyzed per transfection. Immediately before experiments, growth media was removed, and cells were washed two times in Krebs-Ringer solution (KR; 130 mM NaCl, 1.3 mM KCl, 2.2 mM $CaCl_2$, 1.2 mM $MgSO_4$, 1.2 mM KH_2PO_4, 10 mM HEPES, and 1.8 g/L glucose, pH 7.4) buffer. After washing, fresh KR solution was added to the culture dish which was then mounted onto the stage of Nicon Eclipse microscope equipped with an UltraVIEW LCI spinning-disc confocal system (PerkinElmer Life and Analytical Sciences, Boston, MA, USA). Time-resolved quantification of DAT function in single cells was achieved using the fluorescent, high-affinity DAT substrate ASP^+. Use of this fluorescent analog in conjunction with a fluorescently tagged transporter allows monitoring of DAT function in single cells (Schwartz *et al.* 2003, 2006; Mason *et al.* 2005). A within-cell design was used to assess the effects of AEA on ASP^+ uptake. The microscope was focused on the center of a monolayer of cells, and background autofluorescence was determined by collecting an image immediately before replacement of the KR solution containing ASP^+ (10 μM). The rate (slope of the linear accumulation function) of ASP^+ uptake was then measured for 1 min immediately before drug addition. Vehicle or drug was added, and the slope of ASP^+ accumulation was again determined over a 10-min period. Control studies showed that ASP^+ uptake by DAT is linear for 15 min after ASP^+ addition. It is dependent on temperature and extracellular concentrations of Na^+,Cl^-, and is inhibited by DAT substrates (Bolan *et al.* 2007; Zapata *et al.* 2007). Images were collected every 20 s for 13 min to enable capture of ASP^+ fluorescence (excitation, 488 nm; emission, 607–652 nm). The influence of drug pre-treatment on ASP^+ uptake was assessed by comparing the slope values during control conditions (determined 1 min before the addition of drugs) with those acquired 10 min after addition of vehicle or drug.

Image analysis

4-(4-(Dimethylamino)-styryl)-*N*-methylpyridinium fluorescence accumulation was determined from the average pixel intensity at each time point accumulated within the cell using the UltraView software package (PerkinElmer Life and Analytical Sciences), the boundaries of which were determined from a reference picture at the initial time point of YFP fluorescence (indicating the presence of YFP-hDAT at the plasma membrane). Values are expressed as the percentage change in ASP^+ accumulation rate after the addition of drug. Data are expressed as mean ± standard error of means (SEM). Statistical significance at the level of 0.05, was determined by the Student's *t*-test, one or two-way ANOVA using the computer software Origin™ (version 7.1; OriginLab Corp., Northampton, MA, USA) or SPSS. *Post-hoc* analysis was conducted when appropriate using the Bonferonni test. For the nonlinear curve fitting and regression fits of the dose-response and binding data, the computer software Origin™ version 7.1 was used. Fluorescent images were processed using MetaMorph or Image J software (W. Rasband, NIH).

For the analysis of ASP^+ binding data, confocal images were acquired at 0.5-s intervals for 5 s. In each dish, six to eight cells expressing hDAT were analyzed for ASP^+ fluorescent intensity (Arbitrary Fluorescent Unit, AFU) in temporally resolved confocal images. Average

background intensity (fluorescent intensity measured in at least two different regions within a plate that did not contain h-DAT expressing cells) was subtracted and subsequently corrected for the YFP-hDAT expression levels determined by measuring the fluorescent intensity of YFP-hDAT for each cell. The results are presented as corrected arbitrary fluorescent units (CAFU).

DAT redistribution

EM4 cells transiently transfected with YFP-hDAT were mounted on the inverted microscope. After collection of control images (0 min), cells were incubated with AEA (10 μM) or vehicle for 10 min. Confocal z-series sections were taken every 1 μm through the cells (excitation: 488 nm, emission: 525–575 nm) at time 0 and 10 min. Cells were then analyzed using MetaMorph Imaging (Downingtown, PA, USA) software which measures integrated pixel intensity within a cursor defined region. The final (10 min) image was compared to the control (0 min) image and the percent change in fluorescence was used to quantify alterations in intracellular DAT. Single cell analysis was performed by outlining the whole cell and the interior of the cell membrane. The fluorescence of both was measured, with the interior fluorescence expressed as a percentage of the total cell fluorescence. The average of five 1 μm sections from each cell was analyzed to ensure a proper representation of each cell and the ratio values (cytosolic: cell surface) are presented as means ± SEM for each time point. For the nonlinear curve fitting of the data, the Origin version 7.1 (OriginLab Corp., Northampton, MA) was used.

Biotinylation was used to determine whether AEA application alters DAT cell surface expression. Cell surface biotinylation was performed as described previously (Morón *et al.* 2000; Bolan *et al.* 2007) to quantify the amount of plasma membrane DAT protein. EM4 cells (10^5 cells/well) were seeded into 6-well plates containing Dulbecco's modified Eagle's medium/Ham's F-12 medium supplemented with 10% FBS and penicillin (100 U/mL) and streptomycin (100 μg/mL) in an atmosphere of 5% CO_2 and 95% humidified atmosphere at 37°C. After 24 h, cells were transfected with FLAG-hDAT cDNA plasmid (0.1 μg of DAT) using Lipofectamine LTX transfection reagent according to manufacturer's protocol. In all wells, the total amount of plasmid DNA was adjusted with corresponding empty vector. Cells were treated with vehicle (0.1% ethanol) or AEA (10 μM) for 10 min after 48 h of transfection. At the end of the treatment, cells were washed two times with ice-cold phosphate-buffered saline (PBS)/calcium-magnesium buffer (138 mM NaCl, 2.7 mM KCl, 1.5 mM KH_2PO_4, 9.6 mM Na_2H-PO_4, 1 mM $MgCl_2$, and 0.1 mM $CaCl_2$, pH 7.3) and incubated with Sulpho-NHS-SS-Biotin [Sulfosuccinimidyl 2-(biotinamido)-ethyl-1,3-dithiopropionate; 1 mg/mL; Thermo Fisher Scientific, Rockford, IL, USA] in PBS/calcium magnesium buffer for 30 min at 4°C. The reaction was quenched by two washes with ice-cold glycine (100 mm) in PBS/calcium-magnesium buffer and further incubation with glycine at 4°C for 20 min. Then the cells were lysed in 500 μL of radioimmunoprecipitation assay buffer (10 mM Tris–HCl, pH 7.5, 150 mM NaCl, 1 mM EDTA, 0.1% sodium dodecyl sulfate (SDS), 1% Triton X-100, and 0.1% sodium deoxycholic acid) containing protease inhibitors (1 μM pepstatin A, 250 μM phenylmethylsulfonyl fluoride, 1 μg/mL leupeptin, and 1 μg/mL aprotinin) for 1 h at 4°C with constant shaking. Lysates were centrifuged at 25 000 g for 30 min at 4°C, and clear supernatants were incubated with streptavidin beads (100 μL of beads/400 μL of cell lysates from one well) for 1 h at 25°C. Beads were washed three times with radioimmunoprecipitation assay buffer, and bound proteins were eluted with 50 μL of Laemmli buffer (62.5 mM Tris, pH 6.8, 20% glycerol, 2% SDS, 5% β-mercaptoethanol, and 0.01% bromphenol blue) for 30 min at 22°C. Aliquots from total cell lysates (50 μL) and unbound fractions (100 μL) and all (50 μL) of the avidin-bound samples were analyzed by immunoblotting with monoclonal DATspecific rat antibody (Millipore, Billerica, MA, USA). To validate the surface localization of biotinylated DAT protein, blots were striped and reprobed with calnexin antibody (Assay Designs Inc., Ann Arbor, MI, USA). Band intensities were quantified using NIH ImageJ (version 1.32j). DAT

densities from total, non-biotinylated (representing the intracellular pool), and biotinylated (representing the surface pool) fractions were normalized using levels of calnexin in the total extract, and values were averaged across four experiments. The data were analyzed by ANOVA.

[^{3}H]Alanine uptake

EM4cells (plated at 10^{-5} cells per/well) were transfected with hDAT as described above. Uptake assays were conducted as described previously with minor modification (Zapata *et al.* 2007). Briefly, the medium was removed by aspiration, and cells were washed twice with 1.0 mL of Krebs-Ringer-HEPES (KR) buffer pH 7.4 (120 mM NaCl, 4.7 mM KCl, 2.2 mM $CaCl_2$ 10 mM HEPES, 1.2 mM $MgSO_4$, 1.2 mM KH_2PO_4, 5 mM Tris, and 10 mM D- glucose). Cells were then pre-incubated with AEA (10 μM) for 5 min. Uptake was initiated by addition of 50 nM [^{3}H]alanine (82 Ci/mmol, PerkinElmer). After 5 min, uptake was terminated by aspiration of the incubation solution and rapidly washing 3× cold KR assay buffer. Cells were lysed in 0.1% SDS, and accumulated radioactivity was measured (triplicates of 100 μL aliquots of lysed cell preparation) by liquid scintillation counting. For each experiment, non-specific [^{3}H]alanine uptake was defined in parallel experiments as the alanine accumulation in the presence of sodium free buffer and was subtracted from total counts. Sodium free buffer was prepared by replacing NaCl with an equimolar concentration of *N*-methyl-D-glucamine chloride. The pH was adjusted to 7.4 with KOH. Protein concentrations of lysed cell preparations were determined using a protein assay kit (Bradford assay, Bio-Rad, Richmond, CA, USA).

Ca^{2+} imaging

Fluo-3-AM (Invitrogen) was used to monitor changes in intracellular Ca^{2+} levels. Cells were washed twice with 1 mL of KR solution and incubated in 10 μM Fluo 3-AM for 45 min in 37° C. Following pre-treatment, cells were washed three times in 1 mL buffer solution and placed on the stage of an inverted microscope (Nikon Eclipse) equipped with spinning-disc confocal imaging system (PerkinElmer Life and Analytical Sciences). Analysis of fluorescent intensity was performed using the UltraView software package (PerkinElmer Life and Analytical Sciences) and presented as arbitrary fluorescent unit. Background fluorescence were subtracted and the intensity levels were determined before (controls) and during the treatment conditions for each cell. Fluo-3-AM and A23187 were dissolved in dimethylsulfoxide and kept in 10 mM stocks at −20°C.

Results

4-(4-(Dimethylamino)-styryl)-*N*-methylpyridinium rapidly accumulated in the cytoplasm of EM4 cells transfected with YFP-hDAT but not in untransfected cells (Fig. 1a). Consistent with earlier studies (Schwartz *et al*. 2003;Bolan *et al*. 2007), two distinct phases of ASP^+ incorporation were observed (Fig. 1a and b). Rapid (< 1 s; see also Fig. 6b) initial binding of ASP^+ to transporters located on the cell surface was followed by a slower (seconds-minutes) phase of cytoplasmic accumulation of ASP^+ signal. The effect of AEA on the function of hDAT was determined by measuring the rate of ASP^+ accumulation before and after the addition of 10 μM AEA (Fig. 1b). Application of 10 μM AEA for 10 min significantly decreased the rate of ASP^+ accumulation (Fig. 1c: Student's *t*-test, $t = 6.9$; df = 102; $p \leq 0.001$).

The inhibition of ASP^+ accumulation by AEA varied as a function of the duration of AEA exposure time and concentration (Fig. 2). Inhibition was significant within 2 min after AEA addition and was maximal after 10 min (ANOVA, $F_{1,35} = 10.1$; df = 4; $p \leq 0.001$) (Fig. 2a). Fifty percent inhibition ($\tau_{1/2}$) was reached 1.8 ± 0.3 min after AEA addition. Analysis of the slope of ASP^+ accumulation after addition of graded concentrations of AEA (Fig. 2b) revealed an IC_{50} value of 3.2 ± 0.8 μM and a slope value of 1.2.

HEK293 cells do not endogenously express known cannabinoid receptors (e.g., CB1, CB2, GPR55 and GPR119) or vanilloid receptors (Brown 2007). To determine whether other Gi/o type G-proteins mediate that the effect of AEA on ASP^+ accumulation rate, the effect of PTX pre-treatment (100 ng/mL, 14–16 h) on AEA induced inhibition of ASP^+ uptake was assessed in hDAT transfected cells. AEA produced a significant decrease in ASP^+ accumulation relative to controls in vehicle- and PTX-pre-treated cells (Fig. 3a; ANOVA, $F_{3,222} = 19.1$; $p \leq 0.001$). There was no difference between groups in the magnitude of this effect (Bonferroni test, $p > 0.05$).

Anandamide induced release of intracellular Ca^{2+} has been reported in various cell lines (Mombouli *et al*. 1999; Yeh *et al*. 2006). Thus, increased Ca^{2+} (Gnegy *et al*. 2004) and/or the resulting activation of Ca^{2+}-dependent kinase cascades that regulate DAT may underlie AEA-evoked inhibition of DAT function. To test this hypothesis, cells were pre-loaded with the membrane permeable Ca^{2+} indicator Fluo-3-AM (10 μM for 30 min) prior to AEA (10 μM) addition. Application of AEA for 10 min did not alter basal fluorescent intensity (Fig. 3b; Student's *t*-test: $t = 1.72$; df = 10; $p = 0.115$). In contrast, exposure of cells to the 10 μM Ca^{2+} ionophore A23187 (Case *et al*. 1974) for 5 min significantly increased intracellular Ca^{2+} levels (*inset* to Fig. 3b; Student's *t*-test: $t = 17.3$; df = 31; $p \leq 0.001$).

The major chemical moieties contained in AEA are ethanolamine (EA) and arachidonic acid (AA). To determine whether these chemical moieties could by themselves alter the function of hDAT, we examined the effects of EA and AA on the rate of ASP^+ accumulation. Application of EA (30 μM) for 10 min did not significantly alter the rate of ASP^+ accumulation relative to control cells (vehicle: 0.12 ± 7.62; and EA: 1.72 ± 5.51; Student's *t*-test; $t = 0.185$; df = 66; $p = 0.853$). AA is a major metabolite of AEA and modulation of DAT activity by AA has been reported (Zhang and Reith 1996; Chen *et al*. 2003). Thus, the formation of AA may contribute to the effect of AEA on ASP^+ accumulation. ANOVA revealed a significant effect of AA treatment on ASP^+ accumulation (Fig. 4a; ANOVA, $F_{2,123} = 6.71$; $p \leq 0.002$). *Post-hoc* analysis revealed a significant decrease in response to 30 μM (Bonferroni test, $p < 0.05$) but not to 10 μM AA (Bonferroni test, $p \geq 0.05$). In order to test whether the intact AEA or its metabolism to AA mediates the AEA inhibition of ASP^+ uptake rate, the effect of methanandamide (mAEA), a metabolically stable chiral analogue of AEA that is resistant to hydrolytic inactivation by fatty acid amide hydrolase (FAAH; Abadji *et al*. 1994), on the rate of ASP^+ accumulation was also tested. mAEA (10 μM; 10 min), like AEA significantly decreased ASP^+ uptake rate (Fig. 4a; Student's *t*-test, $F_{1,99} = 6.24$; $p \leq 0.001$).

Anandamide is hydrolyzed by FAAH (Cravatt and Lichtman 2002). To determine whether other degradation products of AEA hydrolysis mediate the effects of AEA, the inhibition of ASP^+ uptake by AEA was quantified in the presence and absence of PMSF (0.2 mM), an inhibitor of FAAH (Cravatt and Lichtman 2002). Two factor ANOVA revealed a significant effect of AEA ($F_{1,201} = 58.5$; $p \leq 0.001$) but no significant effect of PMSF ($F_{1,201} = 0.08$; $p \geq 0.7$). Thus, PMSF was ineffective in attenuating the effect of AEA (Fig. 4b). In addition to PMSF, we tested 1 μM URB597, a specific and potent FAAH inhibitor (Kathuria *et al.* 2003), and the cyclooxygenase inhibitor, indomethacin (5 μM) to further investigate the involvement of AEA hydrolysis products in AEA regulation of hDAT (Fig. 4c and d). Two factor ANOVA revealed a significant effect of AEA ($F_{1,161} = 48.2$; $p \leq 0.001$) but no significant effect of URB597 ($F_{1,161} = 1.32$; $p \geq 0.252$). Similarly, in the presence of indomethacin, there was no statistically significant alteration in the AEA inhibition of ASP^+ uptake rate. The extent of AEA inhibition ($F_{1,162} = 45.7$; $p \leq 0.001$) was not statistically different in the presence of indomethacin ($F_{1,161} = 0.99$; $p \geq 0.752$). Thus URB597 and indomethacin were ineffective in attenuating the effect of AEA.

Transporter trafficking allows rapid up- and down-regulation of transporter expression at the cell surface and is one post-translational mechanism implicated in the regulation of DAT

activity (Melikian and Buckley 1999). To determine whether AEA promotes the redistribution of DAT from the membrane to the cytosol, changes in the ratio of surface to intracellular YFP-hDAT fluorescent intensity were assessed at time zero and then again 10 min after addition of AEA (Figs 5 and 6a). This time point was chosen because it was that producing maximal inhibition of ASP^+ uptake. Two factor ANOVA indicated that 10 min after AEA (10 μM) treatment, there is a significant increase in the ratio of intracellular to surface fluorescent intensity (Fig. 6a; 27.1 ± 3.4%; $_{ANOVA\ treatment}$: $F_{1,96} = 15.8$, $p \leq 0.001$, *ANOVA* time: $F_{1,96} = 16.1$, $p \leq 0.001$; $_{ANOVA\ treatmentxtime}$: 15.9, $p \leq 0.001$).

Changes in ASP^+ binding have been used to quantify plasma membrane expression of DAT and other monoamine transporters (Schwartz *et al*. 2003, 2006; Mason *et al*. 2005). Thus, we studied the effect of 10 min AEA (10 μM) pre-incubation on the binding phase of ASP^+ uptake in hDAT expressing cells (Fig. 6b). Binding of ASP^+ reached maximal levels within 0.67 s in control (untreated) cells. Ten min incubation of cells with AEA (10 μM) did not alter the kinetics of ASP^+) binding (vehicle: $\tau_{1/2} = 668 \pm 32$ ms vs. AEA: $\tau_{1/2} = 647 \pm 29$ ms; $_{ANOVA}$, $F_{1,17} = 2.03$; $p = 0.172$). However total binding (B_T) defined by fluorescent intensity significantly decreased (vehicle: $B_T = 0.94 \pm 0.08$ CAFU; AEA: $B_T = 0.73 \pm 0.04$; $_{ANOVA}$, $F_{1,17} = 1891.7$; $p \leq 0.001$).

Biotinylation studies, which permit quantification of cell surface and intracellular DAT, were also conducted in EM4 cells expressing FLAG-hDAT. Consistent with the imaging data, incubation of cells for 10 min with AEA (10 μM) significantly decreased biotinylated DAT (surface) (81 ± 6.7%) and increased non-biotinylated DAT (intracellular) (127 ± 9.3%: $F_{3,12} = 14.8$ $p = 0.00024$), indicating redistribution of DAT from the cell surface to the cytosol (Fig. 7). Treatment with AEA did not alter the total amount of DAT protein as measured by immunoblotting. Less than 0.5% of total calnexin was present in streptavidin-bound fractions, indicating that cells were intact and intracellular proteins were not significantly biotinylated.

To investigate whether AEA regulates hDAT by affecting the lipid-bilayer structure, thereby, non-specifically altering transporter-mediated uptake, we examined the effect of AEA on Na^+-dependent [^{3}H]alanine uptake in hDAT transfected EM4 cells. Ten-minute incubation with 10 μM AEA did not alter [^{3}H]alanine uptake (94.4 ± 2.3% of controls; *ANOVA*, $F_{1,16} = 4.3$; $p = 0.054$; $n = 9$; three experiments performed in triplicate). However, increasing the concentrations of AEA to 30 μM significantly reduced alanine uptake. (76.4 ± 3.1% of controls; $_{ANOVA}$, $F_{1,16} = 56.3$; $p = 0.00012$; $n = 9$, three experiments performed in triplicate).

Discussion

The present studies demonstrate that AEA inhibits the intracellular accumulation of the high affinity, DAT substrate ASP^+ in EM4 cells expressing hDAT. Inhibition of ASP^+ uptake is dependent upon the concentration and duration of AEA exposure and is mimicked by mAEA, a metabolically stable chiral analogue of AEA. The effect of AEA is PTX-insensitive and is not associated with alterations in intracellular Ca^{2+} concentrations. In addition, the inhibition of enzymes such as FAAH, and cyclooxygenase, did not alter the extent of AEA effect on ASP^+ uptake. Quantification of hDAT distribution revealed a significant increase in intracellular hDAT accumulation in response to AEA exposure.

Previous studies have demonstrated the utility of the ASP^+ fluorescent imaging technique for quantifying changes in DAT function in real-time (Schwartz *et al*. 2003, 2006; Mason *et al*. 2005). ASP^+ uptake is saturable, temperature-dependent and decreased by transporter substrates and inhibitors. In contrast, manipulations that increase DAT function increase uptake (Bolan *et al*. 2007; Zapata *et al*. 2007). Together these findings demonstrate that changes in ASP^+ accumulation reflect a transporter mediated process. Furthermore, in contrast to

radioligand techniques, as ASP^+ accumulation is linear for at least 15 min after its addition, a within cell design can be used to monitor time-related alterations in DAT function in living cells.

Exposure of cells to AEA produced a concentration-dependent decrease in ASP^+ uptake. These findings are in accord with a recent electrochemical study (Chen *et al*. 2003). in which inhibition of hDAT function was observed after prolonged drug exposure (15 min) and in response to a higher (80 μM) concentrations (Chen *et al*. 2003). Further, they extend these by showing that the regulation of DAT function occurs at physiological (IC_{50} = 3.2 μM in the present study) AEA concentrations (Howlett *et al*. 2002; Oz 2006). Furthermore, down-regulation of function is rapid occurring within 2 min after AEA addition. PTX pre-treatment did not attenuate the AEA-evoked decrease in ASP^+ uptake. HEK293 cells do not express known cannabinoid receptors (Brown 2007). Therefore, the effects of AEA on DAT function are not because of the activation of cannabinoid receptors or other G_i/G_o dependent G-protein coupled receptors. Indeed, several laboratories have shown that AEA modulates the function of serotonin type 3 (Oz *et al*. 2002; Barann *et al*. 2002; IC_{50} = 0.1–4 νM), nicotinic acetylcholine (Oz *et al*. 2003; Spivak *et al*. 2007; Butt *et al*. 2008; IC_{50} = 0.2–4 μM), and glycine (Lozovaya *et al*. 2005; Hejazi *et al*. 2006; IC_{50} = 0.2–1 μM) receptors by a cannabinoid receptor independent mechanism. Cannabinoid receptor independent modulation of voltage-gated Ca^{2+} (Oz *et al*. 2000; Chemin *et al*. 2001; Fisyunov *et al*. 2006; IC_{50} = 1–10 μM), Na^+ (Nicholson *et al*. 2003; Kim *et al*. 2005; IC_{50} = 10 μM), and K^+ channels (Poling *et al*. 1996; Oz *et al*. 2007; IC_{50} = 0.1–3 μM) has also been reported (for a recent review; Oz 2006). AEA binds to CB1 receptors with an affinity (K_i) ranging from 50 nM to 0.5 μM (Adams *et al*. 1995) when AEA metabolism by FAAH is inhibited by PMSF. However, K_i value of AEA for CB1 receptor increases significantly to 5.4 μM when PMSF is not included in assay conditions (Adams *et al*. 1995), suggesting that AEA regulation of hDAT activity (IC_{50} = 3.2 μM in the present study) can occur at physiologically relevant concentrations.

Anandamide belongs to a class of signaling lipids consisting of amides of long-chain polyunsaturated fatty acids (Howlett *et al*. 2002). Fatty acid-based lipids such as AA modulate DAT function in various expression systems (L'hirondel *et al*. 1995; Zhang and Reith 1996; Chen *et al*. 2003). As AA is a major metabolite of AEA, its formation may have contributed to the AEA-evoked inhibition of ASP^+ uptake. In line with earlier studies, incubation of EM4 cells with AA inhibited the rate of ASP^+ accumulation. However, the concentration (30 μM) of AA producing this effect was 15-folds greater than that for AEA, (i.e. the potency of AA was lower than that of AEA). Therefore, it is unlikely that the AA metabolite was responsible for the AEA-evoked inhibition of ASP^+ uptake. In addition, mAEA, a metabolically stable chiral analogue of AEA that is resistant to hydrolytic inactivation by fatty acid amide hydrolase (Abadji *et al*. 1994) also inhibited DAT function. Importantly, pre-treatment of cells with the non-specific FAAH inhibitor, PMSF, the specific FAAH inhibitor URB597, or the cyclooxygenase inhibitor, indomethacin, did not attenuate the inhibition of ASP^+ accumulation produced by AEA indicating that AEA metabolites do not contribute significantly to the observed effect of AEA.

Anandamide increases intracellular Ca^{2+} levels in several cell lines (Mombouli *et al*. 1999; Yeh *et al*. 2006). Therefore changes in intracellular Ca^{2+} levels and alterations in the activity of calcium–dependent kinase cascades could be one of the mechanisms by which AEA modulates hDAT function (Gnegy *et al*. 2004; Foster *et al*. 2006). Importantly, however, and in accord with other studies conducted in HEK293 cells, use of the membrane permeable Ca^{2+} indicator Fluo-3-AM revealed no change in intracellular Ca^{2+} levels of EM4 cells following AEA treatment (De Petrocellis *et al*. 2000; Jerman *et al*. 2002). Thus, changes in intracellular Ca^{2+} levels do not contribute to the AEA-evoked functional DAT down-regulation observed in the present study. Furthermore, it is unlikely that AEA regulates hDAT activity

by nonspecific perturbations of the lipid bilayer, as Na^+-dependent alanine uptake was not affected by AEA concentrations that significantly decreased ASP^+ accumulation.

Using rotating disk electrode voltammetry, Chen *et al*. (2003) provided evidence that prolonged (15 min) exposure of cells to AEA reduces the V_{max} of DA transport. In contrast, only a small decrease in K_m is observed. To determine whether the inhibition of DAT function by AEA is associated with the redistribution of hDAT from the membrane to the cytosol, we monitored changes in the ratio of surface to intracellular YFP-hDAT fluorescent intensity in vehicle and AEA-treated cells. A significant increase in intracellular fluorescent intensity was observed ten min after AEA addition. However, an AEA concentration (10 μM) producing a ca. 37% decrease in ASP^+ uptake resulted in only a ca. 21% increase in the intracellular/surface ratio. Cell surface biotinylation experiments that used a protocol identical to that of ASP^+ experiments showed that 10 min AEA application significantly decreased cell surface FLAG h-DAT. This decrease was accompanied by a significant increase in intracellular DAT. Similar to analysis of ASP^+ binding to DAT, a modest but a highly significant decrease of cell surface DAT expression was observed. Analogous to our imaging studies, the increase in cytosolic DAT was less than the decrease in ASP+ accumulation. Thus, it is likely that in addition to trafficking, other mechanism(s) contribute to the effects AEA on hDAT function. In this regard, it is interesting to note that AEA and other fatty acid based molecules can directly affect the function of several integral membrane proteins (for reviews; Chalon 2006; Oz 2006) by altering the activation energies required for conformational changes of these membrane proteins (Spivak *et al*. 2007).

Under the conditions of the present study, AEA did not alter the affinity of ASP^+ binding to hDAT. In earlier studies, AEA, at similar concentrations, did not change the binding characteristics of radioligands for DAT (Chen *et al*. 2003; Steffens and Feuerstein 2004), suggesting that AEA may act as an allosteric modulator of hDAT, i.e., it binds to a site topographically distinct from the substrate binding sites on the transporter. These pharmacological properties of AEA and other allosteric modulators are noteworthy in that their effect would not be overcome by the high concentration of endogenous activators (such as neurotransmitters) in the synaptic cleft.

Microdialysis studies have shown that acute administration of AEA increases extracellular DA concentrations in the nucleus accumbens (Solinas *et al*. 2006). Increased extracellular concentrations of DA in this region have been implicated in the rewarding effects of various drugs of abuse (Wise 1987). The results of the present study provide suggestive evidence that AEA-evoked decreases in DAT function and cell surface expression may contribute to the increase in extracellular DA produced by this fatty acid amide. In this regard, it should be noted the increase in extracellular DA produced by AEA in vivo consists of two components. Although the initial increase in DA is reversed by a CB1 receptor antagonist, the second, more prolonged increase in DA is not (Solinas *et al*. 2006).

In conclusion, the present studies demonstrate that AEA decreases hDAT function via a G-protein-independent mechanism. Down-regulation of DAT function is associated with an increase in intracellular DAT expression suggesting that AEA-evoked alterations in transporter trafficking contribute, in part, to the modulation of DAT. These findings add to a growing body of evidence indicating cannabinoid receptor-independent actions of AEA. Additional studies are, however, needed to identify the cellular mechanisms by which AEA modulates DAT and to what extent this action contributes to the regulation of DA transmission function *in-vivo*.

Acknowledgments

This research was supported by the DHHS/NIH/NIDA Intramural Research Program. We thank Drs. V. I. Chefer and J. Meis for their help with statistical analysis and discussion of the data.

Abbreviations used

AA	arachidonic acid
AEA	anandamide
ASP^+	4-(4-(dimethylamino)-styryl)-*N*-methylpyridinium
DA	dopamine
DAT	dopamine transporter
EA	ethanolamine
FAAH	fatty acid amide hydrolase
hDAT	human DAT
KR	Krebs-Ringer
mAEA	methanandamide
PBS	phosphate-buffered saline
PMSF	phenylmethylsulfonyl fluoride
PTX	pertussis toxin
SDS	sodium dodecyl sulfate
YFP	yellow fluorescent protein

References

Abadji V, Lin S, Taha G, Griffin G, Stevenson LA, Pertwee RG, Makriyannis A. (R)-methanandamide: a chiral novel anandamide possessing higher potency and metabolic stability. J. Med. Chem 1994;37:1889–1893. [PubMed: 8021930]

Adams IB, Ryan W, Singer M, Thomas BF, Compton DR, Razdan RK, Martin BR. Evaluation of cannabinoid receptor binding and in vivo activities for anandamide analogs. J. Pharmacol. Exp. Ther 1995;273:1172–1181. [PubMed: 7791088]

Amara SG, Kuhar MJ. Neurotransmitter transporters: recent progress. Annu. Rev. Neurosci 1993;16:73–93. [PubMed: 8096377]

Barann M, Molderings G, Brüss M, Bönisch H, Urban BW, Göthert M. Direct inhibition by cannabinoids of human 5-HT3A receptors: probable involvement of an allosteric modulatory site. Br. J. Pharmacol 2002;137:589–596. [PubMed: 12381672]

Bolan EA, Kivell B, Jaligam V, et al. D2 receptors regulate dopamine transporter function via an extracellular signal-regulated kinases 1 and 2-dependent and phosphoinositide 3 kinase-independent mechanism. Mol. Pharmacol 2007;71:1222–1232. [PubMed: 17267664]

Brown AJ. Novel cannabinoid receptors. Br. J. Pharmacol 2007;152:567–575. [PubMed: 17906678]

Butt C, Alptekin A, Shippenberg T, Oz M. Endogenous cannabinoid anandamide inhibits nicotinic acetylcholine receptor function in mouse thalamic synaptosomes. J. Neurochem 2008;105:1235–1243. [PubMed: 18194436]

Case GD, Vanderkooi JM, Scarpa A. Physical properties of biological membranes determined by the fluorescence of the calcium ionophore A23187. Arch. Biochem. Biophys 1974;162:174–185. [PubMed: 4855487]

Chalon S. Omega-3 fatty acids and monoamine neurotransmission. Prostaglandins Leukot. Essent. Fatty Acids 2006;75:259–269. [PubMed: 16963244]

Chemin J, Monteil A, Perez-Reyes E, Nargeot J, Lory P. Direct inhibition of T-type calcium channels by the endogenous cannabinoid anandamide. EMBO J 2001;20:7033–7040. [PubMed: 11742980]

Chen N, Appell M, Berfield JL, Reith MEA. Inhibition by arachidonic acid and other fatty acids of dopamine uptake at the human dopamine transporter. Eur. J. Pharmacol 2003;478:89–95. [PubMed: 14575792]

Cravatt BF, Lichtman AH. The enzymatic inactivation of the fatty acid amide class of signaling lipids. Chem. Phys. Lipids 2002;121:135–148. [PubMed: 12505696]

De Petrocellis L, Bisogno T, Davis JB, Pertwee RG, Di Marzo V. Overlap between the ligand recognition properties of the anandamide transporter and the VR1 vanilloid receptor: inhibitors of anandamide uptake with negligible capsaicin-like activity. FEBS Lett 2000;483:52–56. [PubMed: 11033355]

Fadda P, Scherma M, Spano MS, Salis P, Melis V, Fattore L, Fratta W. Cannabinoid self-administration increases dopamine release in the nucleus accumbens. Neuroreport 2006;17(15):1629–1632. [PubMed: 17001282]

Fisyunov A, Tsintsadze V, Min R, Burnashev N, Lozovaya NA. Cannabinoids modulate the P-type high voltage-activated calcium currents in Purkinje neurons. J. Neurophysiol 2006;96:1267–1277. [PubMed: 16738209]

Foster JD, Cervinski MA, Gorentla BK, Vaughan RA. Regulation of the dopamine transporter by phosphorylation. Handb. Exp. Pharmacol 2006;175:197–214. [PubMed: 16722237]

Gnegy ME, Khoshbouei H, Berg KA, Javitch JA, Clarke WP, Zhang M, Galli A. Intracellular Ca^{2+} regulates amphetamine-induced dopamine efflux and currents mediated by the human dopamine transporter. Mol. Pharmacol 2004;66:137–1343. [PubMed: 15213305]

Hejazi N, Zhou C, Oz M, Ye HJ, Zhang L. Δ^9-Tetrahydrocannabinol and endogenous cannabinoid anandamide directly potentiate the function of glycine receptors. Mol. Pharmacol 2006;69:991–997. [PubMed: 16332990]

Howlett AC, Barth F, Bonner TI, et al. International Union of Pharmacology. XXVII. Classification of cannabinoid receptors. Pharmacol. Rev 2002;54:161–202. [PubMed: 12037135]

Jerman JC, Gray J, Brough SJ, Ooi L, Owen D, Davis JB, Smart D. Comparison of effects of anandamide at recombinant and endogenous rat vanilloid receptors. Br. J. Anaesth 2002;89:882–887. [PubMed: 12453933]

Kathuria S, Gaetani S, Fegley D, et al. Modulation of anxiety through blockade of anandamide hydrolysis. Nat. Med 2003;9:76–81. [PubMed: 12461523]

Kim HI, Kim TH, Shin YK, Lee CS, Park M, Song JH. Anandamide suppression of Na+ currents in rat dorsal root ganglion neurons. Brain Res 2005;1062:39–47. [PubMed: 16256960]

L'hirondel M, Chéramy A, Godeheu G, Glowinski J. Effects of arachidonic acid on dopamine synthesis, spontaneous release, and uptake in striatal synaptosomes from the rat. J. Neurochem 1995;64:1406–1409. [PubMed: 7861174]

Lozovaya N, Yatsenko N, Beketov A, Tsintsadze T, Burnashev N. Glycine receptors in CNS neurons as a target for nonretrograde action of cannabinoids. J. Neurosci 2005;25:7499–7506. [PubMed: 16107637]

Mason JN, Farmer H, Tomlinson ID, Schwartz JW, Savchenko V, DeFelice LJ, Rosenthal SJ, Blakely RD. Novel fluorescence-based approaches for the study of biogenic amine transporter localization, activity, and regulation. J. Neurosci. Methods 2005;143:3–25. [PubMed: 15763132]

Melikian HE, Buckley KM. Membrane trafficking regulates the activity of the human dopamine transporter. J. Neurosci 1999;19:7699–7710. [PubMed: 10479674]

Mombouli JV, Schaeffer G, Holzmann S, Kostner GM, Graier WF. Anandamide-induced mobilization of cytosolic Ca^{2+} in endothelial cells. Br. J. Pharmacol 1999;126:1593–1600. [PubMed: 10323591]

Morón JA, Zakharova I, Ferrer JV, Merrill GA, Hope B, Lafer EM, Lin LC, Wang JB, Galli A, Shippenberg TS. Mitogen-activated protein kinase regulates dopamine transporter surface expression and dopamine transport capacity. J. Neurosci 2003;23:8480–8488. [PubMed: 13679416]

Nicholson RA, Liao C, Zheng J, David LS, Coyne L, Errington AC, Singh G, Lees G. Sodium channel inhibition by anandamide and synthetic cannabimimetics in brain. Brain Res 2003;978:194–204. [PubMed: 12834914]

Oz M. Receptor-independent actions of cannabinoids on cells membranes: focus on endocannabinoids. Pharmacol. Therap 2006;111:114–144. [PubMed: 16584786]

Oz M, Tchugunova Y, Dunn SMJ. Endogenous cannabinoid anandamide directly inhibits voltage-dependent calcium fluxes in rabbit T-tubule membrane preparations. Eur. J. Pharmacol 2000;404:13–20. [PubMed: 10980258]

Oz M, Zhang L, Morales M. Endogenous cannabinoid, anandamide, acts as a noncompetitive inhibitor on 5-HT_3 receptor-mediated responses in xenopus oocytes. Synapse 2002;46:150–156. [PubMed: 12325042]

Oz M, Ravindran R, Zhang L, Morales M. Endogenous cannabinoid, anandamide inhibits neuronal nicotinic acethylcho-line receptor-mediated responses in xenopus oocytes. J. Pharmacol. Exp. Ther 2003;306:1003–1010. [PubMed: 12766252]

Oz M, Yang KH, Dinc M, Shippenberg TS. The endogenous cannabinoid anandamide inhibits cromakalim-activated K+ currents in follicle-enclosed Xenopus oocytes. J. Pharmacol. Exp. Ther 2007;323:547–554. [PubMed: 17682128]

Poling JS, Rogawski MA, Salem N, Vicini S. Anandamide, an endogenous cannabinoid inhibits Shaker-related voltage-gated K+ channels. Neuropharmacology 1996;35:983–991. [PubMed: 8938728]

Price DA, Owens WA, Gould GG, Frazer A, Roberts JL, Daws LC, Giuffrida A. CB1-independent inhibition of dopamine transporter activity by cannabinoids in mouse dorsal striatum. J. Neurochem 2007;101:389–396. [PubMed: 17250681]

Saunders C, Ferrer JV, Shi L, Chen J, Merrill G, Lamb ME, Leeb-Lundberg LM, Carvelli L, Javitch JA, Galli A. Amphetamine-induced loss of human dopamine transporter activity: an internalization-dependent and cocaine-sensitive mechanism. Proc. Natl Acad. Sci. USA 2000;97:6850–6855. [PubMed: 10823899]

Schwartz JW, Blakely RD, DeFelice LJ. Binding and transport in norepinephrine transporters. Real-time, spatially resolved analysis in single cells using a fluorescent substrate. J. Biol. Chem 2003;278:9768–9777. [PubMed: 12499385]

Schwartz JW, Piston D, DeFelice LJ. Molecular micro-fluorometry: converting arbitrary fluorescence units into absolute molecular concentrations to study binding kinetics and stoichiometry in transporters. Handb. Exp. Pharmacol 2006;175:23–57. [PubMed: 16722229]

Sidló Z, Reggio PH, Rice ME. Inhibition of striatal dopamine release by CB1 receptor activation requires nonsynaptic communication involving GABA, H(2)O(2), and K(ATP) channels. Neurochem. Int 2008;52:80–88. [PubMed: 17767979]

Solinas M, Justinova Z, Goldberg SR, Tanda G. Anandamide administration alone and after inhibition of fatty acid amide hydrolase (FAAH) increases dopamine levels in the nucleus accumbens shell in rats. J. Neurochem 2006;98:408–419. [PubMed: 16805835]

Spivak CE, Lupica CR, Oz M. The endocannabinoid anandamide inhibits the function of alpha4beta2 nicotinic acetylcholine receptors. Mol. Pharmacol 2007;72:1024–1032. [PubMed: 17628012]

Steffens M, Feuerstein TJ. Receptor-independent depression of DA and 5-HT uptake by cannabinoids in rat neocortex – involvement of Na+/K+-ATPase. Neurochem. Int 2004;44:529–538. [PubMed: 15209421]

Tanda G, Pontieri FE, Di Chiara G. Cannabinoid and heroin activation of mesolimbic dopamine transmission by a common mu1 opioid receptor mechanism. Science 1997;276:2048–2050. [PubMed: 9197269]

Wise RA. The role of reward pathways in the development of drug dependence. Pharmacol. Ther 1987;35:227–263. [PubMed: 3321101]

Yeh JH, Cheng HH, Huang CJ, et al. Effect of anandamide on cytosolic Ca(2+) levels and proliferation in canine renal tubular cells. Basic Clin. Pharmacol. Toxicol 2006;98:416–422. [PubMed: 16623868]

Zapata A, Kivell B, Han Y, et al. Regulation of dopamine transporter function and cell surface expression by D3 dopamine receptors. J. Biol. Chem 2007;282:35842–35854. [PubMed: 17923483]

Zhang L, Reith ME. Regulation of the functional activity of the human dopamine transporter by the arachidonic acid pathway. Eur. J. Pharmacol 1996;315:345–354. [PubMed: 8982675]

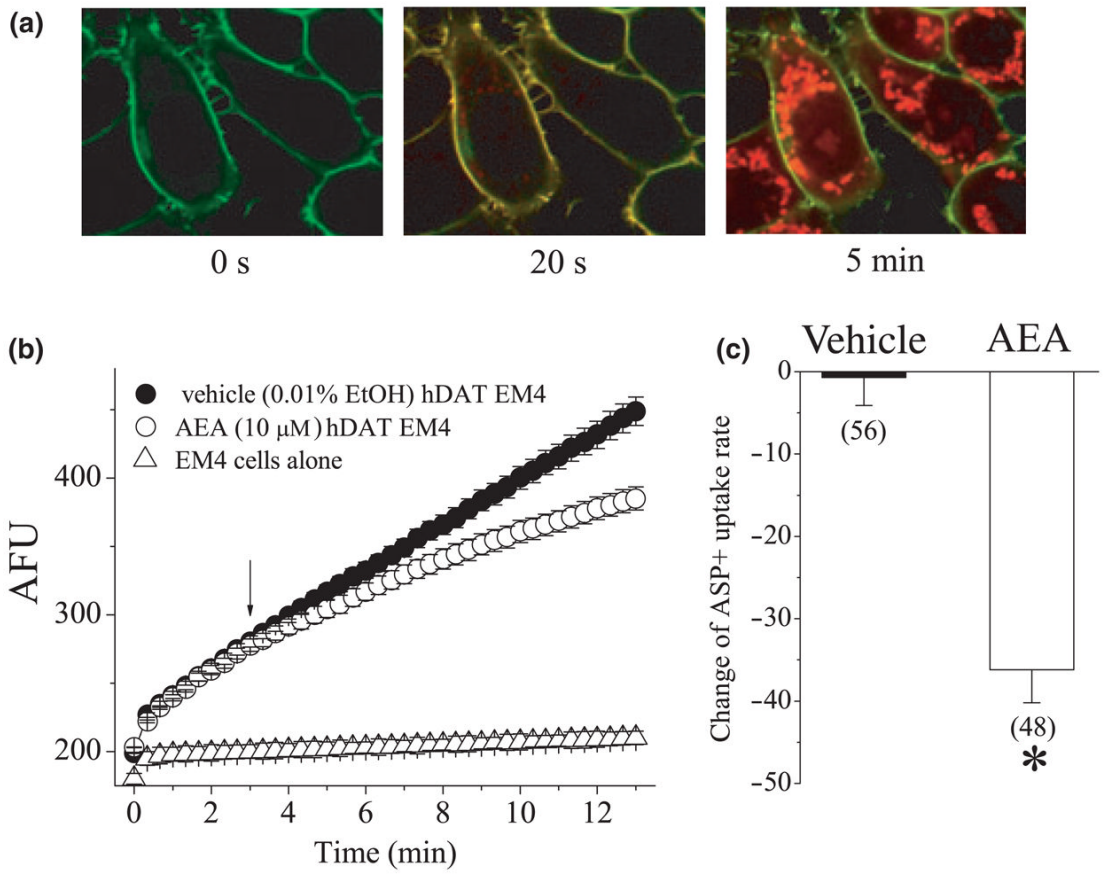

Fig. 1.

The effect of AEA on ASP^+ uptake in EM4 cells transiently transfected with YFP-hDAT. Confocal images presented in panel (a) shows an image of cells expressing YFP-hDAT. YFP-hDAT (green) and ASP^+ (red) localization prior to (time 0: left panel) or 5 (middle panel) and 40 s (right panel) after ASP^+ addition are shown. YFP-DAT is indicated by green fluorescence and ASP^+ by red fluorescence. Co-localization of the two fluorphores is indicated by the merged images (yellow). These images show that ASP^+ rapidly binds to hDAT located on the cell surface followed by a slower phase of intracellular ASP^+ accumulation. (b) Time course of mean ASP^+ uptake in control and AEA-treated cells (n = 9–11 cells/treatment) is shown. Note the initial rapid binding phase after ASP^+ addition followed by the linear uptake phase. Addition of AEA (10 μM) decreases the rate of ASP^+ uptake relative to vehicle (0.001% ethanol) values. The changes in DAT function is presented as the change in the slope of uptake measured for 1 min immediately before and 10 min after AEA addition. Each data point represents the mean ± SEM fluorescent intensity which was calculated as arbitrary fluorescent units (AFU). (c) The bar graph compares changes in the ASP^+ accumulation rates calculated after 10 min application of vehicle (0.001% ethanol) or AEA. The data is from three different experiments. The numbers of cells are presented above each bar. * indicates statistically significant difference at the level of $p < 0.01$.

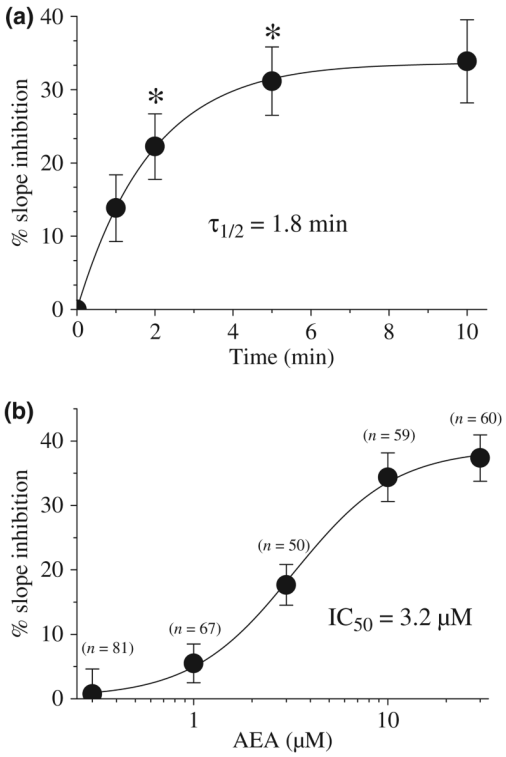

Fig. 2.

AEA inhibits ASP^+ accumulation in a time and concentration-dependent manner. (a) Time course of the effect of AEA on ASP^+ accumulation. Each data point represents the means ± SEM of 9–11 cells. * indicates data points significantly different (at the level of $p < 0.01$) from the mean of the four control measurement taken before the addition of AEA. (b) Concentration-dependent effect of AEA on ASP^+ accumulation. Each concentration of AEA was applied for 10 min and changes in ASP^+ uptake rates are plotted. Data points represent the mean ± SEM of three different experiments. The number of cells used to calculate these values are presented above each data point.

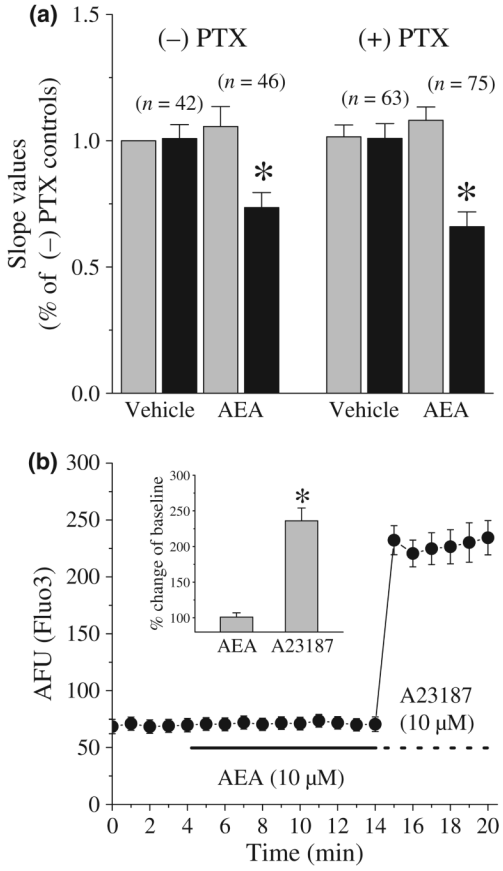

Fig. 3.

Lack of involvement of PTX-sensitive G-proteins or intracellular Ca^{2+} in mediating AEA-evoked functional hDAT regulation. (a) The effects of 10 min application of 10 μM AEA on slope values in control [(−))-PTX] and PTX pre-treated cells [(+) PTX)]. Data points represent the mean ± SEM of three different experiments. The numbers of cells are presented above each data point. * indicates statistically significant difference relative to vehicle at the level of $p < 0.001$. Grey bars for each condition indicate the mean slope values before the addition of vehicle or AEA (pre-treatment slope value). Black bars for each condition represent the mean slope values calculated 10 min after the addition of vehicle or AEA. Slope values normalized to the mean slope value calculated before the vehicle treatment in (−))-PTX group. (b) The effect of 10 min application of 10 μM AEA on intracellular Ca^{2+} levels in Fluo-3-AM (10 μM) loaded cells. Data points indicate the mean ± SEM fluorescent intensity (AFU) from 11 cells. *Inset* shows percent changes in the presence of AEA (10 min, 10 μM) or A23187 (5 min, 10 μM) compared to baseline values at 4 min. * indicates statistically significant difference at the level of $p < 0.01$.

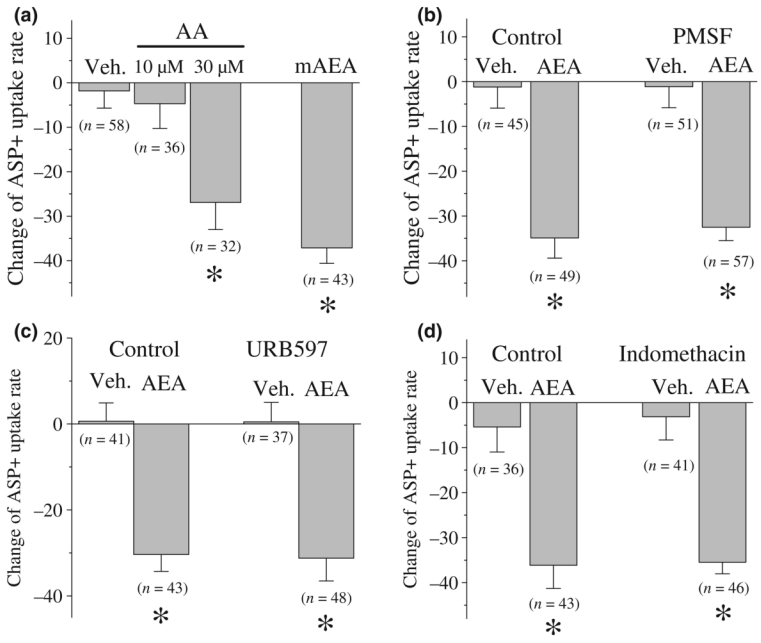

Fig. 4.

AEA inhibition of ASP^+ accumulation rates in EM4 cells expressing hDAT is not mediated by AEA metabolites. (a) Methanandamide (mAEA) but not arachidonic acid (AA) inhibits ASP^+ accumulation at equimolar AEA concentrations. (b) PMSF (0.2 mM) does not alter AEA inhibition of ASP^+ accumulation rates. (c) URB597 (1 μM) does not alter AEA inhibition of ASP^+ accumulation rates. (d) Indomethacin (5 μM) does not alter AEA inhibition of ASP^+ accumulation rates. In the figure, the number of cells analyzed are presented above each bar. Results are expressed as the mean ± SEM Data are from three separate experiments and in each experiment at least three different dishes were analyzed. * indicates statistically significant difference at the level of $p < 0.01$.

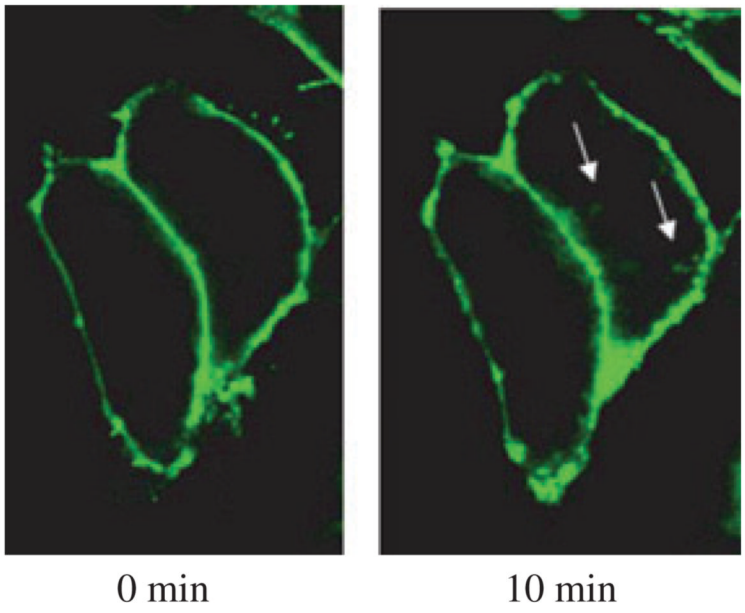

Fig. 5.

Confocal images of EM4 cells expressing YFP-hDAT. Images show the effect of 10-min anandamide treatment on the cellular distribution of YFP-hDAT expression in EM4 cells. The areas with enhanced internalization of YFP-hDAT fluorescence were indicated by arrows in the image shown on the left.

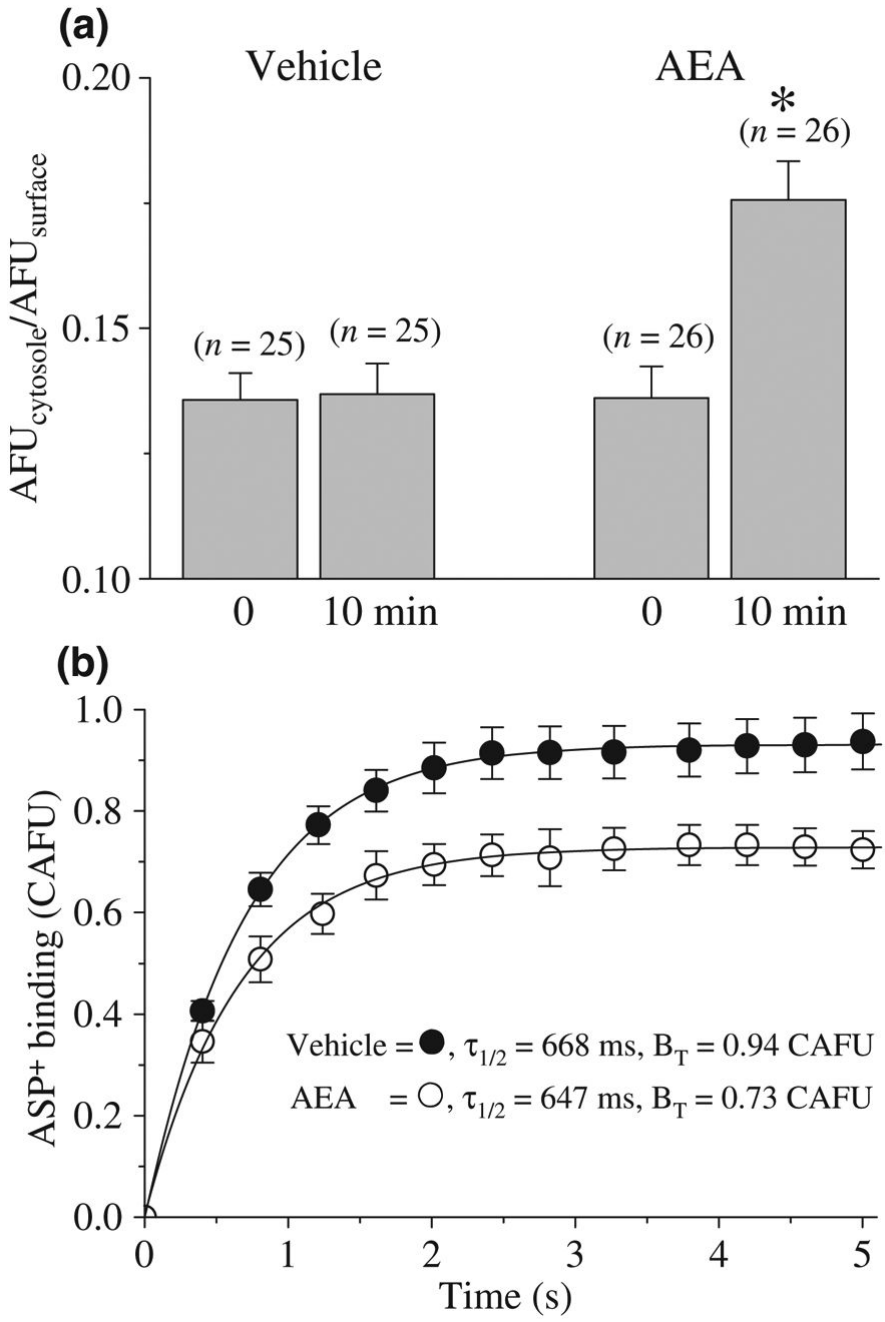

Fig. 6.

Anandamide down-regulates hDAT by increasing the internalization and decreasing surface expression of hDAT in EM4 cells. (a) The ratio of intracellular to surface fluorescent intensity of YFP-hDAT expressed in EM4 cells before and after 10 min pre-incubation with 10 μM AEA. The numbers of cells analyzed are indicated above each bar. Results are expressed as the mean ± SEM. Data are from three separate experiments and in each experiment at least two different dishes were analyzed. * indicates statistically significant difference at the level of $p < 0.01$. (b) AEA pre-incubation decreases membrane ASP^+ fluorescence in the cell surface without altering its affinity for hDAT expressed in EM4 cells. Cells were pre-treated with either vehicle (0.001% ethanol) or 10 μM AEA for 10 min at room temperature (22–24°C) in Krebs

solution. Subsequently, 10 μM ASP^+ (in the continuing presence of vehicle or AEA) was included and the corrected (see *Methods*) ASP^+ fluorescence (excitation, 488 nm; emission, 607–652 nm) intensity (CAFU) was presented as a function of time. B_T: Total binding (maximal CAFU value). $\tau_{1/2}$ = time to reach 50% of maximal CAFU. Each data point is the mean ± SEM from 8 to 11 cells/treatment.

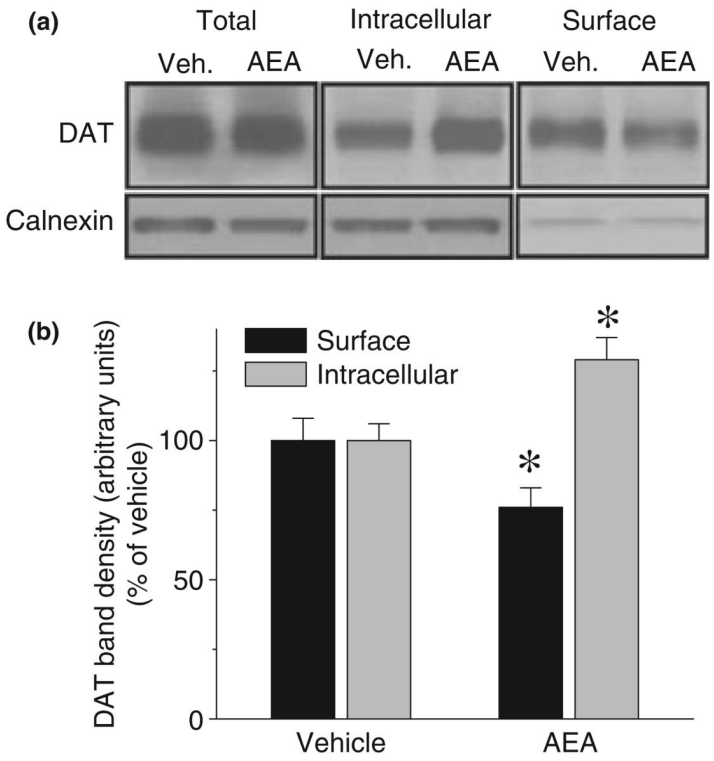

Fig. 7.

AEA application decreases DAT cell surface expression. (a) EM4 cells were transfected with FLAG-hDAT. After 48 h, cells were washed once with KRH buffer and incubated with biotinylating reagent with or without AEA (10 μM) for 10 min. Isolation of biotinylated DAT and detection of DAT were performed as described under *Methods*. Western blots of DAT and calnexin from total lysates, streptavidin beads eluates, and streptavidin beads unbound fractions are shown at the top. Each blot is a representative of four separate experiments. (b) Quantitative analysis of DAT band densities from four experiments (means ± SEM) is shown in bar presentation. *Significant changes in DAT band intensities were compared between vehicle and AEA treatment groups ($p \leq 0.05$, one-way ANOVA with Bonferroni *post hoc* analysis).